doi:10.20944/preprints202206.0362.v1

Article

Research of the Thermal Effect on the Fe-Cr-Al Alloy Foil in the Initial State and with the Supported Secondary Carrier

Bolatbek Khussain [1], Alexandr Brodskiy [1,*], Alexandr Sass [1], Vladimir Yaskevich [1], Irina Shlygina [1], Kenzhegul Rakhmetova [1], Svetlana Tungatarova [1,2*] and Atabek Khussain [1]

[1] D.V. Sokolsky Institute of Fuel, Catalysis and Electrochemistry, 142, Kunaev str., Almaty, 050010, Kazakhstan
[2] al-Farabi Kazakh National University, 71, al-Farabi str., Almaty, 050040 Kazakhstan
* Correspondence: a.brodskiy@ifce.kz; Tel.: +7-777-706-6713; tungatarova58@mail.ru; Tel.: +7-727-291-6632

Abstract: Iron and chromium based alloys have found wide application in various fields of science and technology. Primary carrier based on Fe-Cr-Al alloy is used in block catalysts for high-temperature hydrocarbon conversion, in production of block metal catalysts for neutralization of toxic gases released during operation of internal combustion engines, as well as those present in smoke emissions from enterprises. Influence of thermal action on Fe-Cr-Al alloy foil and stability of secondary carrier on its surface was studied. Elemental composition of the surface layer of X15U5 alloy foil does not remain constant during heating and depends on the thermal treatment mode. Some of the elements come to surface and elemental composition of surface layer can differ significantly from that observed in the bulk of foil sample. This implies the possibility of changing the adhesive and adsorption properties of the foil surface, as well as the need to take this fact into account when supporting a secondary carrier and active phase to the foil. Applied technique of phosphating and supporting a secondary carrier to the foil surface makes it possible to obtain a sufficiently stable coating. There is no shedding of the secondary carrier from foil surface during high-temperature treatment in air.

Keywords: catalytic converters; waste gases; phosphating; oxidation

1. Introduction

Fe-Cr alloys are widely used in various fields of science and technology, in particular, in the processing of materials by pressure, the manufacture of medical instruments, and in the automotive industry. They are regarded as one of the main structural materials for use in nuclear power plants due to their high corrosion resistance and good mechanical properties. In addition, they have no vacancy swelling, which is essential for the technology of fast neutron reactors and thermonuclear reactors [1, 2]. The primary carrier based on the Fe-Cr-Al alloy can be used in block catalysts for high-temperature hydrocarbon conversion, in particular, methane conversion, as well as hydrogen oxidation [3, 4].

Fe-Cr-Al alloys of composition 14 - 23% Cr, 4 - 5% Al are widely used in the form of corrugated tapes in the manufacture of block metal catalysts to neutralize toxic gases released during the operation of internal combustion engines in vehicles, as well as those present in smoke emissions from enterprises [5]. These alloys for use in this capacity were recommended in [6] and the technologies proposed in this work. They remain relevant to the present day.

As a rule, chromium-containing alloys are operated under rather severe temperature conditions. At the same time, during the operation of products made from these alloys, questions arise related to their thermal stability. It has been established that the phenomenon of embrittlement at 475 °C for Fe-Cr alloys (double- and more complex composition) takes place. It is associated with phase transitions inherent in such systems. The data of early works devoted to this issue were discussed in [7].

Subsequently, extensive studies of transformations occurring in chromium-containing alloys at various temperatures and times of thermal action continued [8–19]. It was shown that the separation of the solid solution into regions with different chromium content is possible. The mechanism of this process (spinodal or embryonic) depends on the content of chromium and other metals in the initial alloy, as well as on the heat treatment mode. It was concluded that the change in the mechanical properties of chromium-containing alloys is associated with delamination.

This work is a continuation of the research on study of the influence of thermal effect on Fe-Cr alloys. It was previously shown that it is possible to change the local environment of iron with the formation of regions depleted and enriched in chromium and aluminum atoms under thermal action on the foil of Fe-Cr-Al alloys, which are used as the metal base of catalytic neutralizers of harmful and toxic components of waste (exhaust) gases of motor transport and industrial production [20]. In this case, iron in the nearest coordination spheres can contain a different number of chromium and aluminum atoms.

In this work, the effect of thermal treatment on the surface morphology of the Fe-Cr-Al (X15U5) alloy foil and on the elemental composition of the surface layers was studied. Studies of the physical and chemical characteristics of the primary carrier with the supported secondary carrier in the initial state and in the temperature range from 25 to 900 °C were also carried out. Recent studies have been undertaken to assess the possibility of using this composite as the basis for creating catalytic converters of environmentally harmful components of exhaust gases from internal combustion engines and industrial enterprises with an active phase firmly bound to the surface.

2. Materials and Methods

The studies were carried out on a JSM 6610 LV, JEOL scanning electron microscope with an installed INCA Energy 450 energy-dispersive microanalysis system.

The surface of the foil was pre-treated with a phosphating solution before supporting the secondary carrier (aluminum oxide) for stronger adhesion to the foil metal. After such procedure, drying at room temperature was carried out, or short-term heating in air for 15 min at 400 °C was carried out.

The secondary carrier in the form of a suspension of boehmite (AlOOH) with additions of cerium and aluminum nitrate was supported on the primary carrier - metal foil, after which calcination was carried out at 550 – 600 °C in order to decompose the supported salts and formation of γ-Al_2O_3 from boehmite with a specific surface area of ~ 160 - 180 m^2/g. The used techniques are described in [21-25].

3. Results and Dicussion

3.1. Study of the X15U5 foil surface morphology during thermal treatment

Figures 1-3 show micrographs of the foil surface with different magnifications in the initial state and after thermal treatment. The surface of the X15U5 foil in the initial state is relatively uniform, which is shown in Figure 1. A similar conclusion can be made when the foil is heated for 1 h at 650 °C, Figure 2. At the same time, the homogeneity of the X15U5 foil surface was disturbed when heated at 900 °C for 10 h. This is clearly visible already at magnifications of 1,000 and 3,000 times (Figure 3 b, c). Crystal structures with signs of faceting are clearly visible at magnifications of 10,000 and 25,000 times on the surface of the foil. Data on the relief of the X15U5 foil surface in the initial state and after heat treatment were obtained during further study of the surface morphology. Figures 4 and 5 show the relief of the foil surface in the initial state and after heating at 900 °C for 10 h. The temperature point with the 10 h mark of thermal action at 900 °C was taken, since the surface morphology of the X15U5 foil undergoes significant changes compared to the initial state under these conditions.

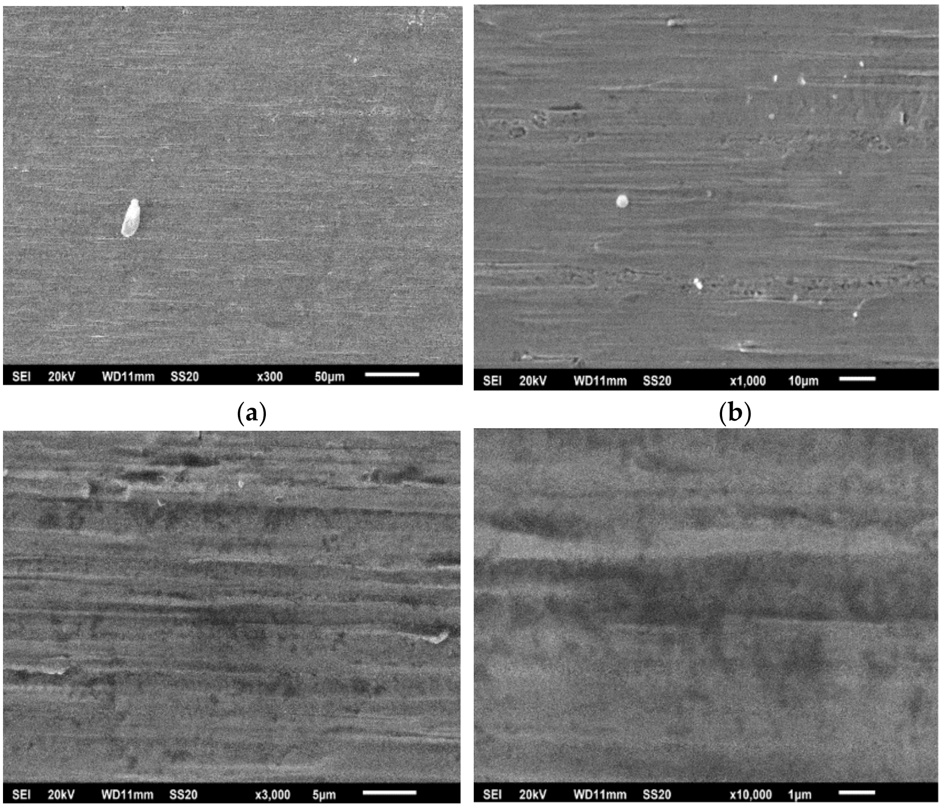

(**a**) (**b**)

(**c**) (**d**)

Figure 1. SEM images of the X15U5 foil surface in the initial state at different magnifications: (**a**) – 300 times, (**b**) – 1,000 times, (**c**) – 3,000 times, (**d**) – 10,000 times.

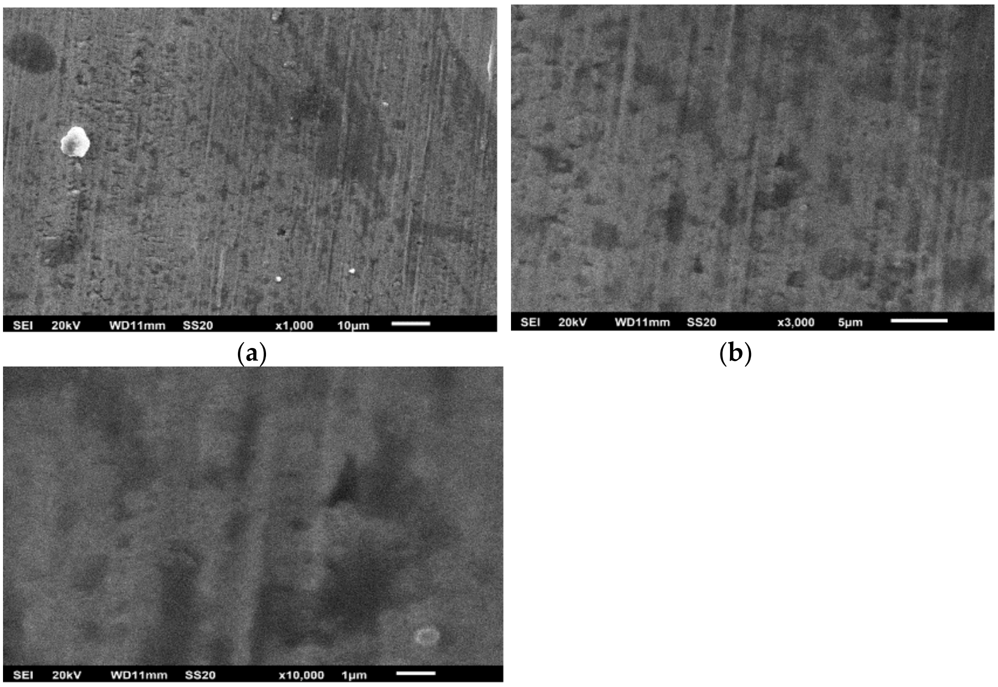

(**a**) (**b**)

(**c**)

Figure 2. SEM images of the X15U5 foil surface at different magnifications after heating at 650 °C for 1 h: (**a**) – 1,000 times, (**b**) – 3,000 times, (**c**) – 10,000 times.

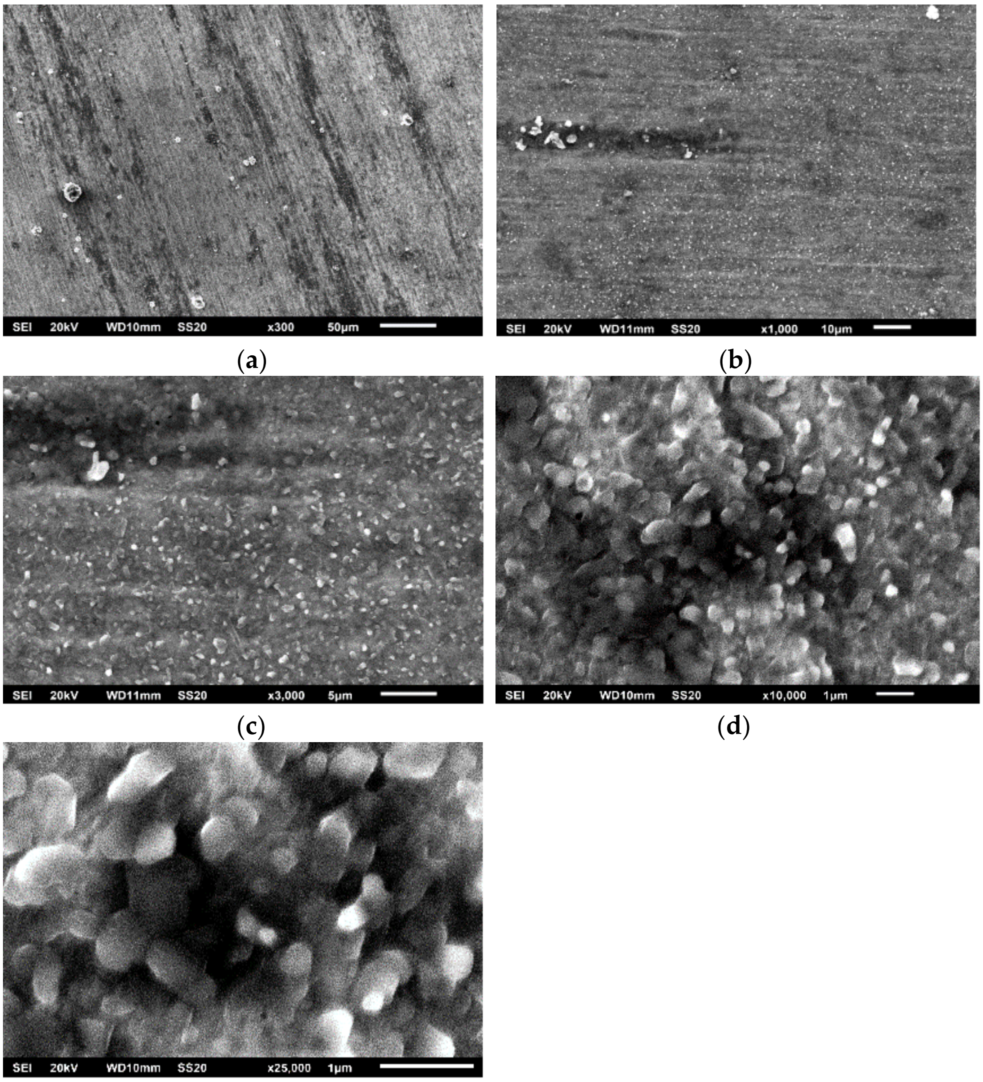

(**a**) (**b**)

(**c**) (**d**)

(**e**)

Figure 3. SEM images of the X15U5 foil surface at different magnifications after heating at 900 °C for 10 h: (**a**) – 300 times, (**b**) – 1,000 times, (**c**) – 3,000 times, (**d**) – 10,000 times, (**e**) – 25,000 times.

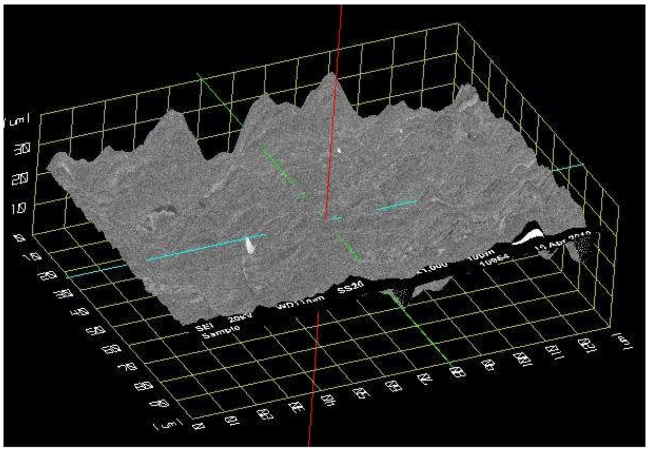

Figure 4. Surface relief of X15U5 alloy foil in the initial state.

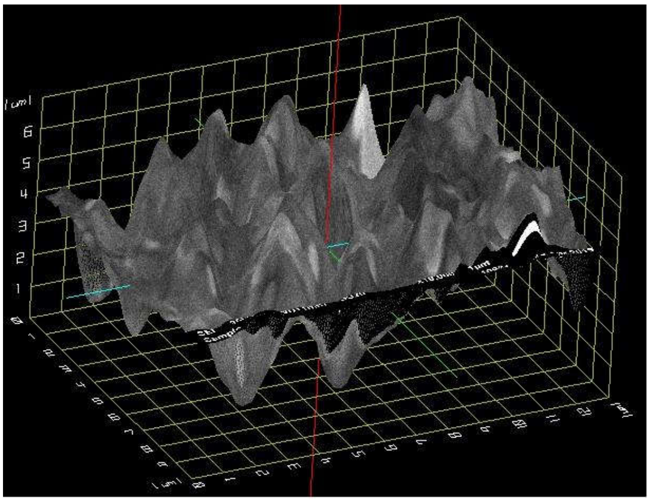

Figure 5. Surface relief of X15U5 alloy foil after heating at 900 °C for 10 h.

Comparison of Figures 4 and 5 shows that the relief of the foil surface after thermal treatment is much more pronounced.

3.2. Investigation of the elemental composition of the X15U5 foil surface before and after heat treatment

Due to the fact that the microanalysis system was on an electron microscope, it was possible to change the depth of the studied surface layer of the foil by varying the accelerating voltage. The penetration depth is about 1.5-2.0 μm at an accelerating voltage of 20 kV, and about 0.5-1.0 μm at an accelerating voltage of 10 kV. Table 1 shows the elemental composition of the Fechral foil surface before and after heating at various accelerating voltages.

Table 1. Elemental composition of the X15U5 foil surface in the initial state and after thermal treatment.

Sample	T (°C)	Accelerating voltage (kV)	Elements (wt %)								
			O	Al	Si	Ti	Cr	Fe	Ni	P	Total
1	25	20	1.78	4.49	0.39	0.27	13.16	79.68	0.22	-	100
		10	1.19	3.03	0.24	0.20	23.22	72.12	-	-	100
2	650, 1 h	20	6.44	5.04	0.38	0.29	12.46	64.53	0.18	0.67	100
		10	7.21	4.91	0.29	0.25	21.52	41.53	-	1.29	100
3	900, 10 h	20	23.95	23.06	0.15	3.52	7.67	41.53	0.12	-	100
		10	32.25	27.49	0.05	10.44	17.63	12.15	-	-	100

Heating of X15U5 foil in an air atmosphere leads to the oxidation process and aluminum coming to the surface, as evidenced by an increase in the content of oxygen and aluminum (Table 1). This occurs most significantly after 10 h of thermal exposure at 900 °C. The same picture is observed for 650 °C, but to a lesser extent. It should be noted a significant coming to the surface of titanium at 900 °C. All of the above phenomena are most clearly manifested at an accelerating voltage of 10 kV, and, consequently, in a thin near-surface layer.

3.3. Physical and chemical characteristics of the primary carrier with the supported secondary carrier

Studies of the physicochemical characteristics of the primary carrier with the supported secondary carrier in the initial state and in the temperature range of 25 – 900 °C were carried out. The foil of the Fe-Cr-Al alloy, as a rule, was subjected to prolonged heating in air at 900 °C for 10 h before supporting of secondary carrier, as was recommended in [6]. The foil was preliminarily phosphated with a phosphating solution before supporting the secondary carrier for stronger adhesion of the foil to the metal.

An intermediate layer of acidic mono- and diphosphates was supported on the surface of a pre-oxidized Fechral foil by treating the foil with a phosphating solution (an aqueous-alcoholic solution of phosphoric acid), followed by drying and heating at 400 °C. Subsequently, acid phosphates bind to boehmite particles with their unsaturated acid groups, forming thermal-resistant and slightly soluble basic phosphates, when impregnated in an aqueous suspension of aluminum oxide-hydroxide (boehmite). The resulting intermediate layer has good adhesion to the metal foil and serves as a basis for further growth of the secondary carrier layer to the required thickness by multiple impregnations with a boehmite suspension with intermediate calcinations at 600 °C.

The method is based on creating an intermediate carrier from aluminum phosphates between metal foil and aluminum oxide. Previously, a metal block from a fat-free Fechral tape was subjected to surface oxidation in air in order to create an oxide coating from foil metals - aluminum, iron, chromium (Figure 6, stage 1). Then the foil was immersed for some time in a phosphating solution consisting of a solution of 33 - 35% phosphoric acid, 7.5 - 8.5% ethanol and 0.7 - 1.0% butanol in water (Figure 6, stage 2). Then the excess of the phosphating solution was removed and the foil was placed in an oven at 400 °C for 20 min. This was done to react the oxide coating with phosphoric acid in order to form acid mono- and disubstituted aluminum and iron phosphates. Excess ortho-phosphoric acid H_3PO_4 at a temperature of 400 °C reversibly transforms into meta-phosphoric acid HPO_3, which, along with acid phosphates, covers the surface of the foil in the form of a thin shiny layer (Figure 6, stage 3). Further application of the oxide layer was carried out by dipping the foil into a suspension of boehmite AlOOH (Figure 6, stage 4), then dried and calcined in an oven at 600 – 650 °C for 1 h (Figure 6, stage 5).

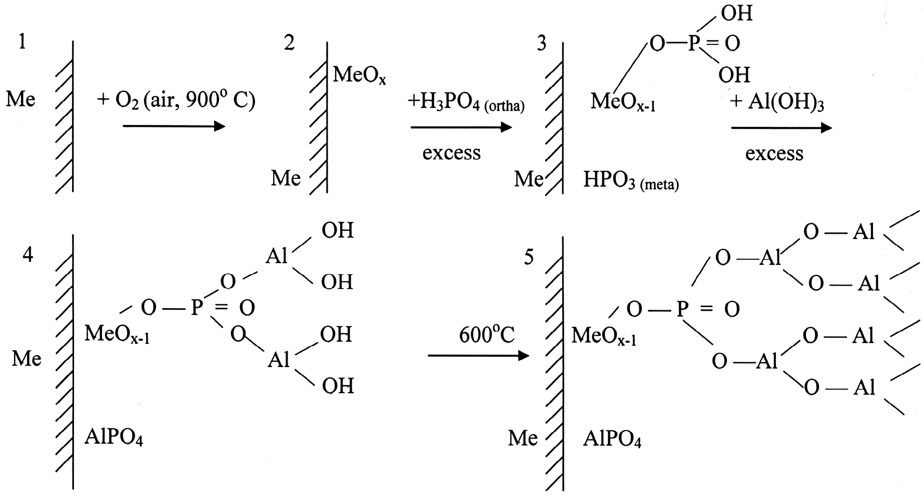

Figure 6. Scheme of the stages of the process of phosphating and supporting aluminum oxide to the pre-oxidized surface of the Fe-Cr-Al foil.

An aqueous suspension of boehmite contains basic hydroxide ($Al(OH)_3$), oxide-hydroxide (AlOOH), and oxide (Al_2O_3). The previously formed acidic metal salts and free phosphoric acid in excess of the listed basic compounds $Al(OH)_3$, AlOOH and Al_2O_3 react with the formation of mixed basic phosphates during drying and calcination. Multibasic phosphoric acid together with multivalent cations (Al^{3+}, Fe^{3+} and Cr^{3+}) create a volumetric spatial structure, forming a strong bond both with the metal through intermediate bonds with phosphate acid groups, and with aluminum oxide from the suspension through the same groups (Figure 6, stage 5). The results obtained for the study of phosphated foil are shown in Table 2.

Table 2. Elemental composition of X15U5 foil in the initial state and after treatment.

Sample	*Accelerating voltage (kV)	Elements (wt %)										
		O	Al	Si	Ti	Cr	Fe	Ni	P	Ca	Mn	Total
4	20	7.93	4.08	0.35	0.28	12.16	72.99	-	1.91	-	0.30	100
	10	7.42	3.50	0.30	0.11	19.36	66.55	-	2.76	-	-	100
5	20	25.06	3.82	0.22	0.18	8.82	50.45	0.16	11.29	-	-	100
	10	29.88	3.63	0.12	-	19.30	29.70	-	17.37	-	-	100
6	20	29.83	24.03	0.16	3.45	6.26	33.42	-	2.62	0.05	0.19	100
	10	40.17	20.76	0.04	8.18	17.02	6.91	-	6.92	-	-	100
7	20	38.78	2.34	0.05	0.10	5.69	31.56	0.12	21.36	-	-	100
	10	29.81	1.46	-	0.03	27.34	20.72	-	20.65	-	-	100
8	20	32.65	4.06	0.12	0.17	7.05	38.62	0.03	17.29	-	-	100
	10	34.40	3.09	-	-	25.25	15.00	-	22.25	-	-	100
9	20	34.27	21.29	0.14	3.61	5.28	27.45	0.17	7.78	-	-	100
	10	43.11	12.24	-	5.69	14.77	6.17	-	18.02	-	-	100

* Accelerating voltage on an electron microscope.
4 - Foil after phosphating and drying at 25 °C.
5 - Foil after heating at 650 °C for 1 h, then phosphating and drying at 25 °C.
6 - Foil after heating at 900 °C for 10 h, then phosphating and drying at 25 °C.
7 - Foil (without preheating) after phosphating and heating at 400 °C for 15 min.
8 - Foil after heating at 650 °C for 1 h, phosphating and heating at 400 °C for 15 min.
9 - Foil after heating at 900 °C for10 h, phosphating and heating at 400 °C for 15 min.

As shown in the previous section, heating the foil in air leads to the oxidation of the foil surface and the release of aluminum to the surface (Table 1). This is especially significant for sample 3; to a lesser extent, this phenomenon is also observed for sample 2 with a lower heating temperature. Sample 7 (Table 2) shows the presence of a large amount of phosphorus-containing phase on the surface of the foil with a simultaneous decrease in the amount of aluminum. The same applies to samples 5 and 8, but the reduction in the amount of aluminum is less significant. A significant amount of the phosphorus-containing phase and aluminium was observed on the surface of sample 9. A small amount (about 2%) of phosphorus-containing phases is present on the surface of sample 4. A large amount of aluminium and a small amount of phosphorus-containing phases are observed on the surface of sample 6. It should be noted that a significant amount of titanium comes to the surface in the case of foil thermal treatment at 900 °C (sample 3, Table 1; samples 6 and 9, Table 2). In addition, thermal treatment leads to the release of a noticeable amount of chromium to the surface with a corresponding depletion of this metal in the inner regions of the foil, as evidenced by the differences in the chromium content at different accelerating voltages (10 and 20 kV). The same applies to titanium and aluminium.

Figure 7 shows SEM images of the X15U5 foil surface with a supported secondary carrier after different thermal treatment modes and at different magnifications, obtained using scanning electron microscopy.

Comparison of the surface of initial samples with the supported secondary carrier (aluminium oxide) with the samples heated for 1 h at 600 and 900 °C shows that at a 30-fold increase, differences in the surface morphology of these samples do not appear. With an increase from 100 to 300 times, it is noticeable that on a sample heated at 900 °C, the existing breaks between blocks of a surface increase somewhat compared to the initial state and thermal treatment at 600 °C. It can be assumed that this is caused by some sintering of the surface of the secondary carrier. At the same time, no traces of even partial shedding of the secondary carrier from the surface of the foil metal were found. Significant differences in the surface structure are not observed at high magnifications. Thus, it can be concluded that the secondary carrier on the foil surface is quite stable and does not crumble during high-temperature treatment in air.

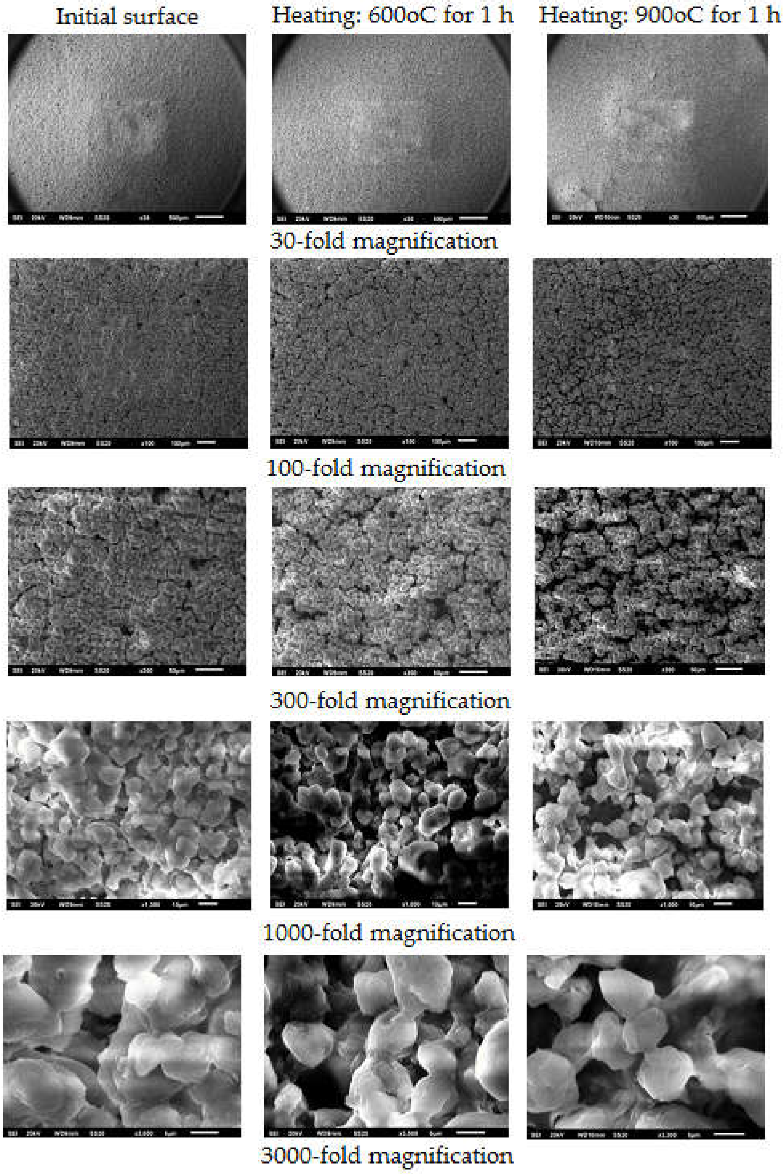

Figure 7. SEM images of the surface of the foil with the supported secondary carrier at various magnifications.

A study of both the integral and local elemental composition of the sample surface was carried out. Table 3 shows the integral elemental composition, and Table 4 shows the local elemental composition of the X15U5 Fechral foil surface after phosphating and heating at 900 °C. Figure 7 shows the areas (points), where local elemental analysis was performed. As follows from Figure 8, points 1 and 2 have a similar morphology. At these points, the elemental composition (Table 4) for all detected elements has only minor differences and is close to the average value of the integral composition of the surface (Table 3). A significant discrepancy between the local elemental composition and the average value of the integral composition of the surface, as well as the local composition at points 1 and 2, is observed in the areas of surface discontinuity - point 3. Based on the data in Table 4, a significant decrease in the content of oxygen, aluminum and phosphorus is observed at point 3. At the same time, the content of chromium, cerium and especially iron increases significantly. This is probably due to the fact that the surface of the primary carrier contains an unfilled portion, in which a high content of metallic chromium and iron is observed (as indicated by a low content of oxygen).

Table 3. Integral elemental composition over the surface of the X15U5 foil sample after phosphating and heating at 900 °C.

Area	Elements (wt%)						
	O	Al	P	Cr	Fe	Ce	Total
1	44.99	38.09	1.53	0.08	0.43	14.88	100
2	43.98	39.06	0.40	0.17	0.63	15.76	100
3	45.07	37.82	1.74	0.14	0.92	14.71	100
Average	44.68	38.32	1.22	0.13	0.53	15.12	100

Accelerating voltage – 20 kV.

Table 4. Local elemental composition over the surface of the X15U5 foil sample after phosphating and heating at 900 °C.

Area	Elements (wt%)						
	O	Al	P	Cr	Fe	Ce	Total
1	28.48	41.99	2.59	0.11	0.58	26.26	100
2	44.87	38.01	1.47	0.10	0.29	15.26	100
3	6.14	7.60	0.34	7.58	36.26	42.07	100

Accelerating voltage – 20 kV.

An almost 3-fold increase in the cerium content relative to the average integral concentration over the surface suggests that when supporting an aqueous suspension of boehmite (AlOOH) containing cerium nitrate, the latter is in the liquid part of the suspension and well wets the foil surface during supporting.

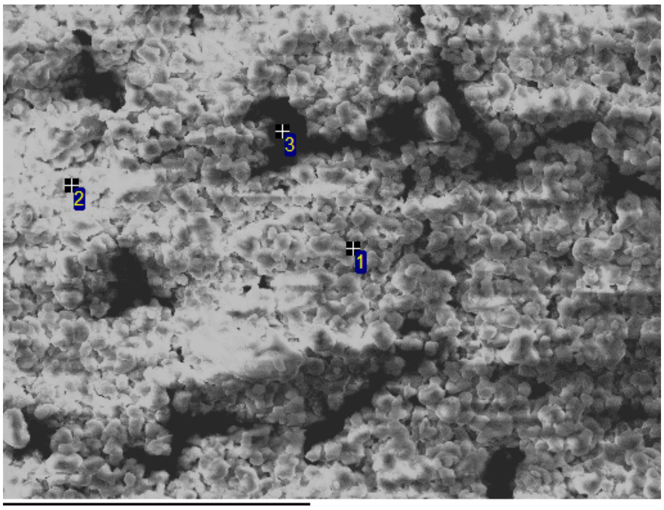

200 μm.

Figure 8. SEM image of the X15U5 foil surface with supported secondary carrier and indication of the regions (points) in which the local elemental composition was determined.

The interlayer between the aluminum oxide coating and the metal surface of the foil is preserved at further stages of the process of supporting the secondary carrier (multiple impregnation, drying and heating even up to 900 °C). This indicates that cerium nitrate is in the form of a highly soluble salt and does not undergo significant hydrolysis in the presence of aluminum oxide - hydroxide.

4. Conclusions

Since a change in the local environment of iron is possible under thermal action [12], this should lead to a change in the mechanical (strength and plastic) characteristics of the Fechral foil, and, consequently, the strength characteristics of the catalyst blocks. In addition, the elemental composition of the surface layer of Fechral X15U5 does not remain constant during heating, but depends on the mode of thermal exposure. This implies the possibility of changing the adhesion and adsorption properties of the surface, which must be taken into account when applying the secondary carrier and active phase to the Fechral foils. The results of the conducted studies showed that the applied technique of phosphating and supporting a secondary carrier to the surface of the Fechral foil makes it possible to obtain a stable coating. The secondary carrier is sufficiently strongly bonded to the foil surface and does not crumble during high-temperature treatment in air.

Shedding or flaking of the secondary carrier was not observed on the blocks of catalytic neutralizers with 20 wt.% supported oxide layer based on the weight of the metal at 1,100 °C heating for 4 h. Shedding and flaking of the aluminum oxide layer when wetting and subsequent drying of the block with the secondary carrier is also not observed. The carrier adhered strongly even when supporting a thick coating of up to 20-30 wt.% of the weight of the metal block. Therefore, it is possible to use this composite with an active phase firmly bound to the primary carrier (Fe-Cr-Al alloy foil) as the basis for creating catalytic neutralizers of environmentally harmful components of exhaust gases from internal combustion engines and industrial enterprises.

Author Contributions: Conceptualization, B.Kh. and A.B.; methodology, A.B. and A.S.; software, A.Kh.; validation, A.S. and V.Y.; investigation, K.R., and A.S.; data curation, A.B. and A.S.; writing—original draft preparation, A.S. and A.B.; writing—review and editing, A.S. and A.B.; visualization, I.Sh.; supervision, K.R. and S.T.; project administration, B.Kh. All authors have read and agreed to the published version of the manuscript.

Funding: This research was funded by Science Committee of the Ministry of Education and Science of the Republic of Kazakhstan, grant number AP08856680.

Data Availability Statement: The data presented in this study are available upon request from the corresponding author.

Acknowledgments: The authors are especially grateful to Academician M. Zhurinov from the National Academy of Sciences of the Republic of Kazakhstan for his support in the research under this work.

Conflicts of Interest: The authors declare no conflict of interest. The funders had no role in the design of the study; in the collection, analyses, or interpretation of data; in the writing of the manuscript; or in the decision to publish the results.

References

1. Pechenkin, V.A.; Molodtsov, V.L.; Ryabov, V.A.; Terentyev, D. On the radiation-induced segregation: contribution of interstitial mechanism in Fe-Cr alloys. *Journal of Nuclear Materials* **2012**, *433*, 372-377.
2. Chen, D.; Kimura, A.; Han, W. Correlation of Fe/Cr phase decomposition process and age-hardening in Fe–15Cr ferritic alloys. *Journal of Nuclear Materials* **2014**, *455*, 436-439.
3. Almyasheva, O.V.; Vlasov, E.A.; Khabenskii, V.B.; Gusarov, V.V. Thermal stability and catalytic properties of the composite amorphous Al_2O_3-nanocrystals ZrO_2. *Russian Journal of Applied Chemistry* **2009**, *82*, 217-221.
4. Maltseva, N.V.; Postnov, A.Yu.; Lavrishcheva, S.A.; Kirshin, A.I. Block Al-Zr-Ce catalysts for hydrogen oxidation. *Izvestiya SPbGTI(TU)* **2016**, *32*, 28–33. (in Rus.).
5. Gilmundinov, Sh.A.; Sassykova, L.R.; Telbaeva, M.M. Block catalysts for solving environmental problems of the Republic of Kazakhstan *News of the National Academy of Sciences of the Republic of Kazakhstan. Series of Chemistry and Technology* **2011**, *3, 55-57.* (in Rus.).
6. Plemyannikova, N.M.; Gorokhov, N.A.; Zhukov, L.L. Alloy for catalyst carrier in exhaust gas neutralization. *Journal of Ferrous Metallurgy* **1987**, *5*, 45-46. (in Rus.).
7. Litvinov, V.S.; Karakishev, S.D.; Ovchinnikov, V.V. Nuclear Gamma Resonance Spectroscopy of Alloys, Metallurgy: Moscow, Russia, 1982; p. 143. (in Rus.).
8. Trindade, B.; Vilar, R. Influence of nickel on 475 ^{o}C embrittlement of Fe-Cr-Ni alloys: Mössbauer effect staudy // *Hyperfine Interactions* **1991**, *66*, 351-358.

9. Kuwano, H,; Ishikawa, Y.; Yoshimura, T.; Hamaguchi, Y. Characterization of the spinodal decomposition of Fe-Cr alloys by Mössbauer spectroscopy. *Hyperfine Interact* **1991**, *69*, 501-504.
10. Danoix, F.; Auge, P. Atom probe studies of the Fe-Cr system and stainless steels aged at intermediate temperature: a review. *Materials Characterization* **2000**, *44*, 177-201.
11. Taniguchi, S.; Andoh, A. Improvement in the oxidation resistance of an Al- deposited Fe-Cr-Al foil by preoxidation. *Oxidation of Metals* **2002,** *58*, 545-562.
12. Bonny, G.; Terentyev, D.; Malerba, L.; Lukon, E. The hardening of iron– chromium alloys under thermal ageing: An atomistic study. *Journal of Nuclear Materials* **2009**, *385*, 278-283.
13. Xu, X.; Odqvist, J.; Colliander, M.H.; King, S.; Thuvander, M.; Steuwer, A.; Hedström, P. Effect of cooling rate after solution treatment on subsequent phase separation during aging of Fe-Cr alloys: A small-angle neutron scattering study. *Acta Materialia* **2017**, *134*, 221-229.
14. Dimyati, A.; Penkalla, H.J.; Untoro, P.; Naumenko, D.; Quadakkers, W.J.; Mayer, J. High-temperature oxidation of FeCrAl alloys: the effect of Mg incorporation into the alumina scale. *Zeitschrift für Metallkunde* **2003**, *94*, 180-187.
15. Molodtsov, V.L.; Ryabov, V.A.; Pechenkin, V.A.; Terentyev, D. On the radiation-induced segregation: contribution of interstitial mechanism in Fe-Cr alloys. *Journal of Nuclear Materials*, **2013**, *433*, 372-377.
16. Israelsson, N.; Unocic, K.A.; Hellström, K.; Svensson, J.E.; Johansson, L.G. Cyclic corrosion and chlorination of an FeCrAl alloy in the presence of KCl. *Oxidation of Metals* **2015**, *84*, 269-290.
17. Chen, H.; Kim, S.H.; Long, C.; Kim, C.; Jang, C. Oxidation behavior of high-strength FeCrAl alloys in a high temperature supercritical carbon dioxide environment. *Progress in Natural Science: Materials International* **2018**, *28*, 731-739.
18. Eklund, J.; Jönsson, B.; Persdotter, A.; Liske, J.; Svensson, J.E.; Jonsson, T. The influence of silicon on the corrosion properties of FeCrAl model alloys in oxidizing environments at 600 °C. *Corrosion Science* **2018**, *144*, 266-276.
19. Rebak, R.B.; Gupta, V.K.; Larsen, M. Oxidation characteristics of two FeCrAl alloys in air and steam from 800 °C to 1,300 °C. *JOM* **2018**, *70*, 1484-1492.
20. Khussain, B.Kh.; Brodskiy, A.R.; Yaskevich, V.I.; Zhurinov, M.Zh.; Abilmagzhanov, A.Z. Investigation of the influence of the thermal effects on the FeCrAl alloys Kh15Yu5 and Kh23Yu5. *EurAsian Journal of BioSciences* **2019**, *13*, 687-694.
21. Sassykova, L.R.; Rakhmetova, K.S.; Massenova, A.T.; Gilmundinov, Sh. A.; Basheva, Zh.T.; Kalykberdiyev, M.; Ussenov, A. The degree of conversion of nitrogen oxide and the resistance of block catalysts to poisons in exhaust gases purging processes. *News of the National Academy of Sciences of the Republic of Kazakhstan. Series of Chemistry and Technology* **2015**, *5*, 89 – 96. (in Rus.).
22. Sassykova, L.R.; Nalibayeva, A.; Gilmundinov Sh. A. Synthesis and testing of catalysts on metal blocks for purging exhaust gases in actual operating conditions. *News of the National Academy of Sciences of the Republic of Kazakhstan. Series of Chemistry and Technology* **2016**, *5*, 118 -125. (in Rus.).
23. Sass, A.S.; Sabitova, I. Zh.; Massenova, A.T.; Kenzin, N.R.; Rakhmetova, K.S.; Ussenov, A.K.; Komashko, L.V.; Yaskevich, V.I. Development of block-type platinum catalysts for deep oxidation of hydrocarbons. Communication 1. *News of the National Academy of Sciences of the Republic of Kazakhstan. Series of Chemistry and Technology* **2017**, *3*, 73-78. (in Rus.).
24. Sass, A.S.; Sabitova, I. Zh.; Massenova, A.T.; Kenzin, N.R.; Rakhmetova, K.S.; Ussenov, A.K.; Kurguzikova, S.A. Development of block-type platinum catalysts for deep oxidation of hydrocarbons. Communication 2. *News of the National Academy of Sciences of the Republic of Kazakhstan. Series of Chemistry and Technology* **2017**, *3*, 81-86. (in Rus.).
25. Khussain, B.Kh.; Zhurinov, M.Zh.; Abilmagzhanov, A.Z.; Sass, A.S.; Teltayev, B.B. Nanostructural catalysts for neutralization of toxic gases in industry. *News of the National Academy of Sciences of the Republic of Kazakhstan. Series Chemistry and Technology* **2020,** *439*, 116 – 122.